Enhancing the performance of Praziquantel: an approach using Crystal Engineering and Mechanosynthesis

Margarida Gonçalves Susana[1*]

[1]Centro de Química Estrutural, Instituto Superior Técnico, Universidade de Lisboa, Av. Rovisco Pais, 1, 1049-001 Lisboa, Portugal;

*margaridasusana98@gmail.com

Abstract

Praziquantel (PZQ) is an anthelmintic drug used for the treatment of parasitic diseases that is considered essential by the WHO. Despite its importance, some of its physicochemical properties are poor. Applying the principles of crystal engineering and supramolecular chemistry, and using mechanochemistry as the main synthetic technique, the goal of this work was to obtain cocrystals of PZQ with organic coformers, in order to enhance its physicochemical properties, namely solubility and stability. Cocrystals of PZQ with nine different coformers, salicylic (SAL), 4-aminosalicylic (4-ASA), vanillic (VAN), 4-hydroxybenzoic (4-HBZ), 5-hydroxyisophthalic (5-HIP), muconic (MUC), 1,2,4,5-benzenetetracarboxylic (BTC), 3-hydroxybenzoic (3-HBZ), and trimesic (TRI) acids, were synthetized by liquid-assisted grinding. BTC and 3-HBZ provided cocrystals in a stoichiometric ratio of 2:1, TRI gave cocrystals with 1:2 ratio, while the remaining coformers reacted in a 1:1 stoichiometry. In all cocrystals, the supramolecular interactions in the crystal structures revealed dominant hydrogen bonding patterns, especially through O-H···O bonds established between PZQ' carbonyl moiety and the carboxylic groups of the coformers. The cocrystals obtained were characterized by powder and single-crystal X-ray diffraction (PXRD and SCXRD, respectively), FTIR-ATR, combined DSC-TGA and by Hot Stage Microscopy. Shelf stability tests have shown that the PZQ cocrystals with 5-HIP and TRI were stable for at least two months, while the cocrystals with SAL, BTC, VAN, 3-HBZ and 4-HBZ were stable for at least three months. These stable forms were tested under 83 and 90 % RH controlled humidity environment showing stability in both environments for 70 days, in the case of SAL, BTC, VAN, 3-HBZ and 4-HBZ, and for 48 h, for 5-HIP and TRI. Preliminary empirical solubility tests were also performed, indicating that the novel cocrystals were more soluble in water than PZQ alone.

Keywords

Praziquantel, supramolecular synthons, cocrystals, mechanochemistry

Introduction

The focus of drug development is to produce a drug with optimal physicochemical properties, high biological activity, and improved therapeutical applications[1]. However, despite the high number of successfully discovered new drugs, a significant part of them presents poor biopharmaceutical properties[2]. Thus, a promising sustainable development pathway is to find new formulations of already marketed drugs with the aim of improving their pharmaceutical properties. Amongst the most common techniques to solve drug property related issues are the development of pharmaceutical cocrystals, salts, solvates/ hydrates, and polymorphs of active pharmaceutical ingredients (API)[1,3]. Pharmaceutical cocrystals, which have been assuming a particularly relevant role in this quest, can be described as multicomponent crystalline materials constituted of an API combined with at least one coformer[4,5], being this coformer Generally Regarded As Safe (GRAS)[6]. The assembly between cocrystal's components is done *via* non-covalent interactions, mostly hydrogen bonds (H-bonds)[1], based on the principles of crystal engineering and supramolecular chemistry.

Praziquantel (PZQ), in Figure 1, is an anthelmintic drug for the treatment of parasitic diseases caused by cestodes and trematodes used in human and veterinary medicine. This drug is the only one commercially available to treat schistosomiasis in

humans, an infection caused by flatworms, and, for that reason, it is included in the World Health Organization (WHO) Model List of Essential Drugs[7-8].

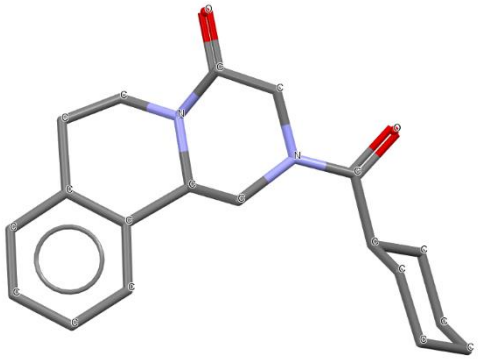

Figure 1 Structure of (R,S)-PZQ. H atoms were omitted for clarity.

PZQ is classified as a BCS class II drug, due to its poor aqueous solubility (0.40 mg/ mL at 25 °C) and high permeability. It is synthesized and administered in the racemic form, *(RS)*-PZQ, and it must be administered in high doses (600 mg tablets for humans)[7,9-10]. Therefore, the use of PZQ is limited, hence the need to discover and identify new solid forms, such as polymorphs, hydrates or cocrystals, to improve its weak physicochemical and biopharmaceutical properties is needed[7,11].

Despite the need to enhance PZQ's properties, there are not many cocrystals of this API reported yet. In 2013, Herbert Höpfl and coworkers[7] reported seven cocrystals of PZQ with fumaric, adipic, maleic, oxalic, succinic, malonic and glutaric acids. In February 2021, Li Zhang *et al.*[12] published their work where they report cocrystals of PZQ with three flavonols. Finally, and already during this work, René de Gelder[11] reported twelve cocrystals of PZQ, in which some of the coformers they predicted to be formed were the ones being explored in this work: salicylic, 4-aminosalicylic, 4-hydroxybenzoic and vanillic acids.

The goal of the work presented herein is to obtain cocrystals of PZQ with different coformers prone to establish supramolecular interactions with the carbonyl moiety of PZQ. The main synthetic technique used during the work was mechanochemistry that is nowadays a common approach for the synthesis of cocrystals[13,14].Liquid-assisted grinding (LAG) was the method used, where a small amount (η= 0-2 µL mg^{-1}) of solvent is introduced into a milling jar along with the reactants and the balls, allowing to control the chemical selectivity[15,16]. The ultimate goal of the work was to enhance the physicochemical properties of PZQ (namely solubility), what has been achieved.

Results and Discussion

Screening experiments

In PZQ, only the oxygen atoms of the carbonyl groups function as H-bond acceptors despite this drug also having two amide groups. Considering the structures of the reported PZQ cocrystals[7], all coformers studied present benzene rings with at least one carboxylic group; muconic acid, an aliphatic dicarboxylic acid is an exception. In addition, 4-aminosalicylic acid is the only coformer with NH_2 groups that provided cocrystals with PZQ. Figure 2 illustrates the successful results of the screening experiments.

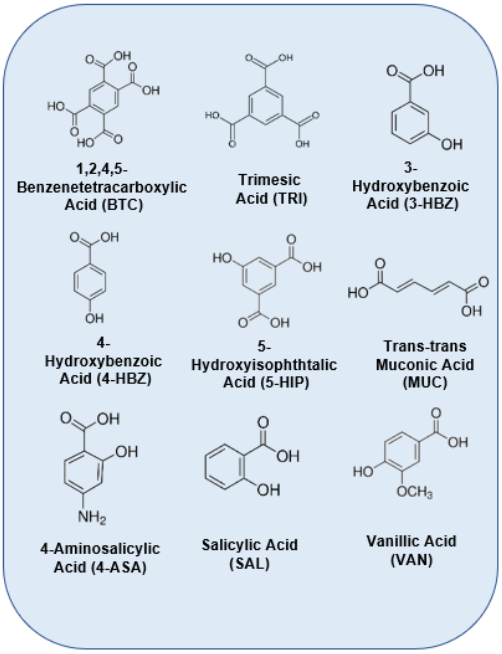

Figure 2 Coformers that provided cocrystals when combined with PZQ.

PXRD Analysis

By comparing the PXRD patterns of the final products with those of PZQ and respective coformer, we can infer that LAG experiments with SAL, 4-ASA, VAN, 4-HBZ, 5-HIP and MUC produced 1:1 cocrystals, BTC and 3-HBZ 2:1 cocrystals, while TRI gave 1:2 cocrystals. Comparing the experimental diffractograms with the simulated from SCXRD, the formation of PZQ·SAL, PZQ·4-ASA, PZQ·VAN, PZQ·4-HBZ, PZQ·BTC 2:1, PZQ·3-HBZ 2:1 and PZQ·TRI 1:2 cocrystals was confirmed. PZQ·5-HIP and PZQ·MUC did not provided single crystals, but there was indication for novel compounds. As example, Figure 3 depicts the PXRD pattern of the products obtained in the reaction of PZQ with 3-HBZ, where the SCXRD data confirmed the 2:1 ratio of the final compound.

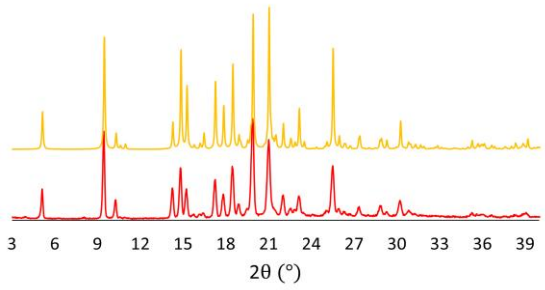

Figure 3 PXRD patterns for PZQ·3-HBZ with 2:1 stoichiometry (in red) and the pattern of PZQ·3-HBZ 2:1 simulated from the SCXRD analysis (in yellow).

Supramolecular Structural Results

Apart from PZQ·VAN and PZQ·TRI 1:2, which crystallize in the monoclinic crystal system, all single crystals obtained crystalized in the triclinic space group. The asymmetric unit of PZQ·VAN and PZQ·4-HBZ are constituted by one molecule of PZQ and one of the respective coformer each, while PZQ·BTC 2:1 and PZQ·3-HBZ 2:1 cocrystals consists of two molecules of API for one of coformer. PZQ·4-ASA is a cocrystal solvate, containing one molecule of PZQ, one of coformer and one acetonitrile solvent molecule. PZQ·SAL is a cocrystal hydrate, whose asymmetric unit consists of one PZQ molecule, one of SAL and one of water, while PZQ·TRI 1:2 is a cocrystal dihydrate containing one molecule of PZQ, two of TRI and two of water.

The supramolecular arrangement in PZQ·VAN and PZQ·4-HBZ cocrystals is based on O-H···O H-bonds between PZQ and the carboxylic moieties of the respective coformers. This type of H-bonds is also maintained in PZQ·SAL together with O-H···O H-bonds between COOH and water molecules. In PZQ·4-ASA additional N-H···N are formed between 4-ASA and acetonitrile as well as N-H···O H-bonds between PZQ and the coformer, while the O-H···O H-bonds between PZQ and the carboxylic acid are also present. These four cocrystals, PZQ·VAN, PZQ·4-HBZ, PZQ·SAL and PZQ·4-ASA, were reported by René de Gelder[11] in May 2021, during this work, and, therefore, the full data collection for structural elucidation from SCXRD was not carried out. The CIFs deposited at Cambridge Structural Database (CSD) with the refcodes AVEJAP (PZQ·VAN), AVEJIX (PZQ·4-HBZ), AVEHER (PZQ·SAL) and AVEJOD (PZQ·4-ASA) were used to describe the crystal structures[11].

From the single crystals obtained, PZQ·BTC 2:1, PZQ·3-HBZ 2:1, and PZQ·TRI 1:2 were not reported yet. The supramolecular arrangement in PZQ·BTC 2:1, in Figure 4, shows intermolecular O-H···O H-bonds between the molecules, evidencing the $R_4^4(28)$ synthons formed between the carboxylic moieties of BTC and the C=O from PZQ. BTC has four carboxylic groups in its structure, being that each of these moieties bond to one molecule of API.

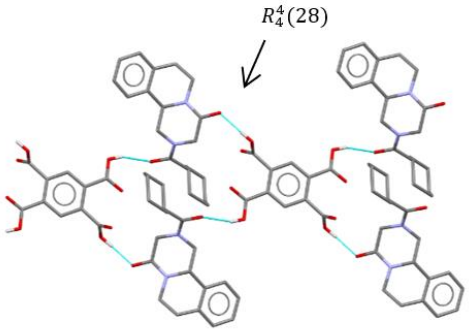

Figure 4 Supramolecular arrangement in PZQ·BTC 2:1. All non-contact H atoms were omitted for clarity.

In PZQ·3-HBZ 2:1, in Figure 5, the interactions are similar to those of PZQ·BTC 2:1, showing dominant O-H···O H-bonds between the carbonyl from the amide of PZQ and the COOH and the hydroxyl group of 3-HBZ.

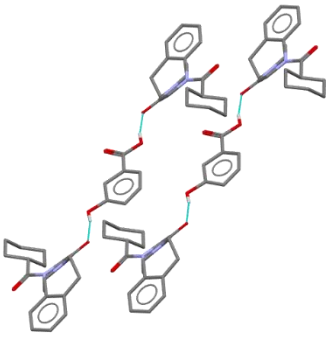

Figure 5 Supramolecular arrangement in PZQ·3-HBZ 2:1. All non-contact H atoms were omitted for clarity.

In PZQ·TRI 1:2, presented in Figure 6, this type of H-bonds are maintained together with O-H···O H-bonds between C=O from PZQ and the water molecules, evidencing the $R_2^2(8)$ synthons formed between the carboxylic moieties from TRI. TRI has the capacity to form three $R_2^2(8)$ synthons between each other, however, in this cocrystal dihydrate, only two are formed while the other is disrupted to give rise to the interaction with PZQ and the water molecules.

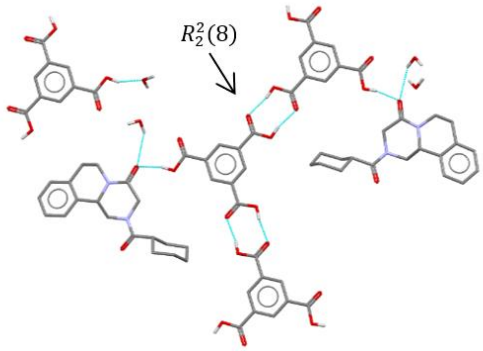

Figure 6 Supramolecular arrangement in PZQ·TRI 1:2. All non-contact H atoms were omitted for clarity.

IR Spectroscopy

The structural elucidation was complemented by FTIR-ATR analysis. The most relevant IR bands for the new cocrystals are given in Table 1.

Table 1 List of relevant IR bands for the new cocrystals.

Cocrystals	Cocrystal $\tilde{\nu}_{C=O}$ (amide)	Cocrystal $\tilde{\nu}_{C=O}$ (COOH)	H-bonds
PZQ·SAL	1592/ 1577	1670	3531-3461
PZQ·4-ASA	1635/ 1610	-	3232
PZQ·BTC 2:1	1592/ 1585	1708	3021-2852
PZQ·VAN	1637	1672	3004-2840
PZQ·3-HBZ 2:1	1631/ 1612	1714	-
PZQ·4-HBZ	1618/ 1591	1704	3209
PZQ·TRI 1:2	1618/ 1602	1720/ 1695	3064-3012

As expected, the changes in the position of the bands observed were related to the carbonyl stretching vibrations of the amide groups present in PZQ's structure as well as the carbonyl stretching of the carboxylic groups common to the coformers. The band for $\tilde{\nu}_{C=O}$ (amide) in PZQ at 1630/1620 cm^{-1}, and for $\tilde{\nu}_{C=O}$ (COOH) in the coformers at approx. 1650-1700 cm^{-1} are slightly shifted in the cocrystals' spectra due to the supramolecular interactions formed. The presence of broad bands for larger wavenumbers in the cocrystals was also expected since they are assembled *via* H-bonds. The results from PZQ·4-ASA, in Figure 7, show some additional peaks at 3444 and 3336 cm^{-1} related to the NH stretch of the aromatic primary amide present in the coformer, as well as a peak at 2252 cm^{-1} derived from the aliphatic nitrile of the acetonitrile present in the cocrystal solvate.

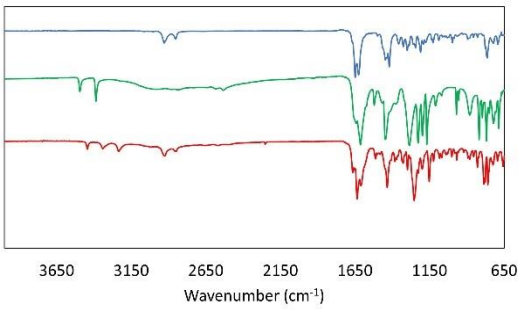

Figure 7 IR spectra of PZQ (in blue), 4-ASA (in green) and PZQ·4-ASA (in red).

Thermal Studies: DSC-TGA and HSM

DSC-TGA as well as HSM experiments were performed with the aim to evaluate the thermal stability of the cocrystals studied. These studies were not performed for PZQ·TRI 1:2, PZQ·5-HIP and PZQ·MUC due to lack of stability or purity of the compounds. Table 2 presents the melting and decomposition temperatures of the cocrystals obtained by DSC-TGA.

Table 2 Melting and decomposition temperatures of the cocrystals studied.

Cocrystals	T_{max} melting (° C)	Decomposition Start (° C)
PZQ·SAL	90.25	218
PZQ·4-ASA	160.3	-
PZQ·BTC 2:1	210.13	210.13
PZQ·VAN	137.3	215
PZQ·3-HBZ 2:1	105	230
PZQ·4-HBZ	152.4	221.7

For PZQ·SAL, in Figure 8, in addition to the endothermic peak representative of the cocrystal melting, at approx. 90.25 °C, a mass loss of 3.84 % would be expected to show at around 100 °C, in the TGA, corresponding to the loss of the water molecule, since the cocrystal is an hydrated form.

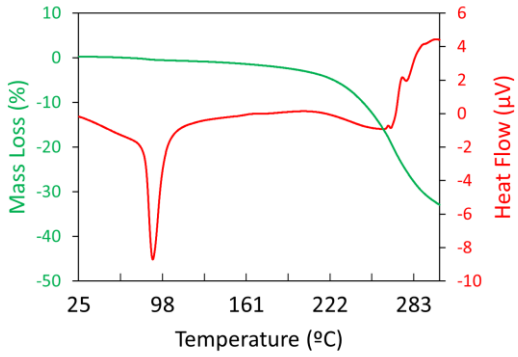

Figure 8 DSC (in red) and TGA (in green) for PZQ·SAL.

Also, for PZQ·4-ASA, in Figure 9, it is possible to observe a phase transition at 96.6 °C, with a mass loss of 4.5% (8.1 % *vs* 4.5 %), correspondent to the release of the molecule of acetonitrile present in the cocrystal solvate structure.

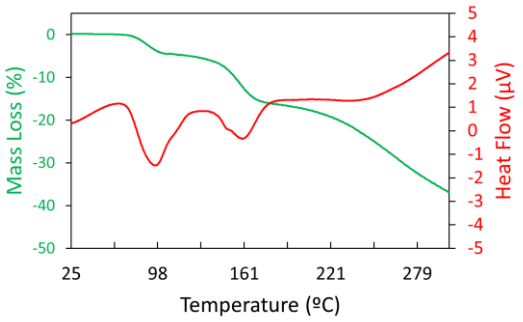

Figure 9 DSC (in red) and TGA (in green) for PZQ·4-ASA.

HSM experiments were also performed for these cocrystals, expect for PZQ·4-ASA. Results showed a good agreement with the data obtained by DSC-TGA. In the case of PZQ·SAL (Figure 10) the release of the water molecules is visible. The observed difference in the temperature of the events is due to the experimental conditions.

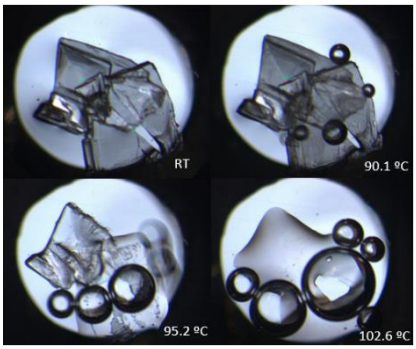

Figure 10 HSM images for PZQ·SAL.

Stability Studies

PZQ·4-ASA and PZQ·MUC shown to be unstable on-shelf after three and two months after being synthetized, respectively (Figure 11). All the other new crystalline forms were considered stable on-shelf up to three months.

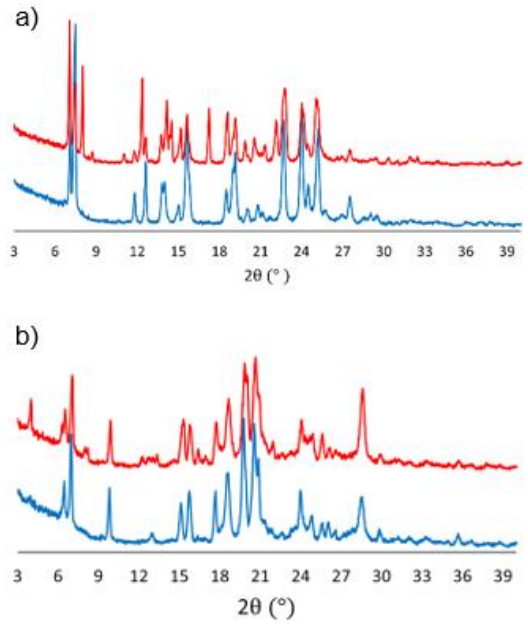

Figure 11 (a) Comparison of PXRD patterns for PZQ·4-ASA (in blue) and PZQ·4-ASA after 3 months (in red) on-shelf. (b) Comparison of PXRD patterns for PZQ·MUC (in blue) and PZQ·MUC after 2 months (in red) on-shelf.

In addition, powder stability was also tested at controlled room humidity environments, at storing under 90 and 83 % RH content. PZQ·SAL, PZQ·BTC 2:1, PZQ·VAN, PZQ·3-HBZ 2:1 and PZQ·4-HBZ were stable for both humidity environments for 70 days. PZQ·TRI 1:2 and PZQ·5-HIP were analyzed only after 24 and 48 h within the desiccators, being considered stable in both environments. Despite the lack of stability on-shelf, PZQ·4-ASA room humidity stability, studies at 90 and 83% RH were also performed, showing alterations in the PXRD patterns after 24 h for both environments (Figure 12). Stability in these environments was not studied for PZQ·MUC due to being unstable on shelf.

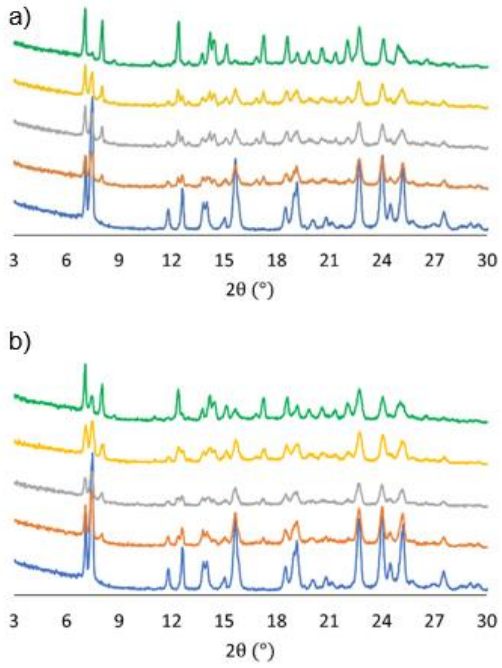

Figure 12 (a) Stability comparison under 90 % RH and (b) under 83 % RH for PZQ·4-ASA (in blue) for 1 (in orange), 2 (in grey), 3 (in yellow) and 7 days (in green).

Solubility Studies

Solubility was evaluated using an empirical method to compare pure PZQ and the new compounds that proved to be stable on-shelf. The preliminary results, presented in Figure 13, show that the aqueous solution of PZQ is the most turbid (lower stability) in comparison with the cocrystals' solutions. PZQ·5-HIP appears to be the most soluble of the studied forms since it required half the amount of water to show the same turbidness. The solubility for 3-HBZ 1:1 was also tested, because it provided a new form different from the single-crystals obtained and, despite not being in a pure form, it showed to also improve the solubility of PZQ. As for the other solutions, it is not possible to rank them from the most to the less soluble because they have the same clarity. Anyway, these data prove that the new PZQ cocrystals can, indeed, enhance the aqueous solubility of the API. Nevertheless, it is crucial to perform further investigations carrying out HPLC studies to fully characterize the solubility profile of these new PZQ forms.

Figure 13 Solubility comparison for PZQ, PZQ·3-HBZ 2:1, PZQ·4-HBZ, PZQ·TRI 1:2, PZQ·VAN, PZQ·SAL, PZQ·BTC 2:1, PZQ·3-HBZ 1:1 and PZQ·5-HIP (from left to right).

Experimental Section

Materials

All reagents and solvents used work were purchased from Sigma-Aldrich, Fluka, Alfa Aesar and TCI Chemicals and used as received without further purification.

Cocrystal Preparation

LAG experiments were performed in a Retsch MM400 mixer mill operated at a frequency of 25 Hz during 30 min (expect for PZQ·VAN that took 45 min) using snap closure stainless steel grinding jars of 10 mL. 40 µL of solvent (acetonitrile, expect for PZQ·3-HBZ in which acetone was used) and two stainless steel balls of 7 mm each were added to approximately 200 mg of mixture with the correspondent stoichiometric ratio of PZQ·coformer: 1:1 for SAL, 4-ASA, VAN, 4-HBZ, 5-HIP and MUC, 2:1 for BTC and 3-HBZ and 1:2 for TRI.

Single-Crystal Growth

The new cocrystal crystalline forms of PZQ suitable for SCXRD analysis were obtained by two different methods: (ii) Cocrystals of PZQ·SAL, PZQ·4-ASA, PZQ·BTC, PZQ·VAN, PZQ·3-HBZ and PZQ·4-HBZ were obtained by recrystallization of the LAG product in saturated solutions (PZQ·SAL and PZQ·VAN- water and ethanol, PZQ·4-ASA, PZQ·BTC and PZQ·4-HBZ- acetonitrile, PZQ·3-HBZ- acetone and diethyl ether), that were left to crystallize at room temperature by slow evaporation of the solvent; (ii) PZQ·TRI 1:2 single crystals (promoting the solution reaction), dissolving an equimolar mixture of PZQ (30.3 mg) and TRI (20.8 mg) in a solvent solution (in a mixture of 3.5 mL of ethyl acetate and 3.5 mL of n-heptane, heated up to 40 ºC and stirred for approx. 20 min), with the reaction yielding directly single crystals.

Instrumental

***Powder X-ray Diffraction (PXRD)*:** data were collected on a D8 Advance Bruker AXS θ-2θ, diffractometer equipped with a LYNXEYE-XE detector, copper radiation source (Cu Kα, λ =1.5406 Å), operated at 40 kV and 40 mA. Data was collected in the 3-60° range in 2θ, with a step size of 0.02°. Throughout the measurements, nickel filter was used in the data collection. MERCURY 2021 2.0[17] was used to obtain the calculated diffraction patterns from SCXRD data.

Single-Crystal X-Ray Diffraction (SCXRD): Crystals suitable for single X-ray diffraction studies were mounted on a loop with Fomblin© protective oil. Data were collected on A Bruker AXS-KAPPA D8 - QUEST, with graphite-monochromated radiation (Mo Kα, λ=0.71073 Å), at 293 K. X-ray generator was operated at 50 kV and 30 mA and APEX3 program monitored the data collections. Data were corrected for Lorentzian polarization and absorption effects using SAINT[18] and SADABS[19] programs. SHELXT 2014/4[20] was used for structure solution and SHELXL 2014/7[20] was used for full matrix least-squares refinement on F^2. These two programs are included in the WINGX-Version 2014.1[21] program package. A full-matrix least-squares refinement was used for the non-hydrogen atoms with anisotropic thermal parameters. Hydrogens were insert in idealized positions and allowed to refine in the parent carbon atom, except the water hydrogen atoms that were located from the electron density map and the distances were restrained. MERCURY 2021.2.0[17] was used for packing diagrams. PLATON[22] was used for determination of hydrogen bond interactions. Crystallographic details are given in Table 3.

Table 3 Crystallographic data of PZQ·BTC 2:1, PZQ·3-HBZ 2:1 and PZQ·TRI 1:2.

	PZQ·BTC 2:1	**PZQ·3-HBZ 2:1**	**PZQ·TRI 1:2**
Chemical Formula	$C_{42}H_{54}N_4O_{12}$	$C_{45}H_{54}N_4O_7$	$C_{37}H_{35}N_2O_{16}$
Molecular weight (g/mol)	878.95	762.92	737.67
Crystal form, colour	Block-shape, colorless	Plate-like, colorless	Plate-like, colorless
Crystal size (mm)	0.180 x 0.100 x 0.080	-	-
Crystal system	Triclinic	Triclinic	Monoclinic
Space group	*P-1*	*P1*	*C 2/c*
a (Å)	9.5037(1)	6.2139(6)	16.49(4)
b (Å)	10.5666(13)	9.6836(9)	34.59(8)
c (Å)	12.6738(13)	17.2147(17)	14.00(4)
α (°)	108.196(4)	90.689(4)	90
β (°)	103.340(4)	95.127(4)	116.82(6)
γ (°)	106.032(3)	105.817(4)	90
V (Å^3)	1089.8(2)	991.93(17)	7128(30)
Z	1	1	8
d (mg.cm^{-3})	1.339	1.277	1.423
μ (mm^{-1})	0.097	0.086	0.113
θ range (°)	1.804-26.500	2.187-33.293	2.011-25.838
Reflections collected/unique	48372/ 4467	73675/ 15154	562937/ 6806
R_{int}	0.1112	0.2206	0.1630
GoF	1.024	0.967	1.231
Final R indices[a,b] [$I > 2\sigma(I)$]	R_1=0.1023, wR_2=0.2465	R_1=0.0749, wR_2=0.1722	R_1=0.1252, wR_2=0.3535

Fourier Transform Infrared Spectroscopy with Attenuated Total Reflectance (FTIR-ATR): The FTIR spectra were obtained in reflectance mode using a Thermo Nicolet 6700 spectrometer with attenuated total reflectance (ATR). The measurements were recorded in the range of 650-4000 cm $^{-1}$, 64 scans, and applying background and atmosphere correction when needed.

Differential Scanning Calorimetry (DSC) and Thermogravimetric Analysis (TGA): Combined TGA-DSC measurements were carried out on a SETARAM TG-DTA 92 thermobalance under nitrogen flow with a heating rate of 10 °C /min. The samples weights were in the range 10-20 mg.

Hot-Stage Microscopy (HSM): Hot-stage experiments were carried out using a Linkam TP94 device connected to a Linkam LTS350 platinum plate. Images were collected, via the imaging software Cell, with an Olympus B061 microscope. The crystals were placed on an oil drop to allow a better visualization of solvent or decomposition products release.

Stability Studies: The new forms obtained by mechanochemistry (LAG) were placed in two different desiccators: one containing a saturated solution of KNO_3 and the other containing a saturated solution of NaCl. These solutions were able to maintain the environment of the desiccators with a RH content of 90% and 83%, respectively, during the experiments.

Solubility Studies: Preliminary solubility studies were carried out by dissolving ~10 mg of each new crystalline forms in water, gradually added, starting by 1 mL, and stirred until complete dissolution. The amount of water added, and the clarity of the solutions allowed the estimation of an empirical relative solubility behavior when compared to PZQ alone.

Conclusions

Nine different cocrystals of PZQ were mechanochemically synthetized by LAG. The cocrystals were structurally characterized and presented different stoichiometries: 1:1 for PZQ·SAL, PZQ·4-ASA, PZQ·4-HBZ, PZQ·VAN, PZQ·5-HIP and PZQ·MUC, 2:1 for PZQ·3-HBZ and PZQ·BTC and 1:2 for PZQ·TRI. From these nine cocrystals, only PZQ·5-HIP and PZQ·MUC did not provided single crystals suitable for SCXRD analysis and structural elucidation. PZQ·SAL and PZQ·TRI 1:2 formed cocrystal hydrates and dihydrates, respectively, while PZQ·4-ASA provided a cocrystal solvate with acetonitrile.

Except for PZQ·MUC, that was not pure, all cocrystals were characterized by FTIR-ATR, confirming the dominant hydrogen bonding patterns suggested by SCXRD data, specially through O-H···O H-bonds between PZQ carbonyl moiety and the carboxylic acid groups of the coformers. In PZQ·4-ASA cocrystal solvate, additional N-H···N and N-H···O H-bonds were noted. Thermal characterization was performed by DSC-TGA and HSM for the most relevant cocrystals, showing an increase in the melting point for PZQ·4-ASA and PZQ·BTC 2:1 when

compared to the literature value[23] for PZQ alone (136 °C).

Regarding shelf stability, only PZQ·4-ASA and PZQ·MUC were not stable on-shelf after three and two months after being synthetized, respectively. PZQ·SAL, PZQ·BTC, PZQ·VAN, PZQ·3-HBZ 2:1 and PZQ·BTC 2:1 cocrystals were stable on-shelf for three months, while PZQ·TRI 1:2 and PZQ·5-HIP were stable on-shelf for two months. Regarding RH stability, only PZQ·4-ASA was considered unstable in environments with 90 and 83 % RH content. Importantly, preliminary solubility studies indicate that aqueous solubility is increase by the formation of cocrystals.

Acknowledgements

Authors acknowledge the funding from Fundação para a Ciência e a Tecnologia, (projects UIDB/00100/2020, UIDP/00100/2020, and PTDC/QUI-OUT/30988/2017, and FEDER, Portugal 2020 and Lisboa2020 (project LISBOA-01-0145-FEDER-030988), as well as to COST Action CA18112.

Prof. M. Teresa Duarte and Dr. Vânia André for their guidance and support during this work.

Professor Hermínio Diogo and Dr. Auguste Fernandes are acknowledged for DSC-TGA data.

References

[1] Pindelska, E.; Sokal, A.; Kolodziejski, W. Pharmaceutical Cocrystals, Salts And Polymorphs: Advanced Characterization Techniques. *Advanced Drug Delivery Reviews* 2017, *117*, 111-146.

[2] Kalepu, S.; Nekkanti, V. Insoluble Drug Delivery Strategies: Review Of Recent Advances And Business Prospects. *Acta Pharmaceutica Sinica B* 2015, *5* (5), 442-453.

[3] Schultheiss, N.; Newman, A. Pharmaceutical Cocrystals And Their Physicochemical Properties. *Crystal Growth & Design* 2009, *9* (6), 2950-2967.

[4] Shemchuk, O.; André, V.; Duarte, M.; Braga, D.; Grepioni, F. Mechanochemical Preparation Of Molecular And Ionic Co-Crystals Of The Hormone Melatonin. *CrystEngComm* 2019, *21* (18), 2949-2954.

[5] Duggirala, N.; Perry, M.; Almarsson, Ö.; Zaworotko, M. Pharmaceutical Cocrystals: Along The Path To Improved Medicines. *Chemical Communications* 2016, *52* (4), 640-655.

[6] Generally Recognized as Safe (GRAS). https://www.fda.gov/food/food-ingredients-packaging/generally-recognized-safe-gras (accessed Oct 8, 2021).

[7] Espinosa-Lara, J.; Guzman-Villanueva, D.; Arenas-García, J.; Herrera-Ruiz, D.; Rivera-Islas, J.; Román-Bravo, P.; Morales-Rojas, H.; Höpfl, H. Cocrystals Of Active Pharmaceutical Ingredients—Praziquantel In Combination With Oxalic, Malonic, Succinic, Maleic, Fumaric, Glutaric, Adipic, And Pimelic Acids. *Crystal Growth & Design* 2012, *13* (1), 169-185.

[8] Andrews, P.; Thomas, H.; Pohlke, R.; Seubert, J. Praziquantel. *Medicinal Research Reviews* 1983, *3* (2), 147-200.

[9] Woelfle, M.; Seerden, J.; de Gooijer, J.; Pouwer, K.; Olliaro, P.; Todd, M. Resolution Of Praziquantel. *PLoS Neglected Tropical Diseases* 2011, *5* (9), e1260.

[10] Šagud, I.; Zanolla, D.; Perissutti, B.; Passerini, N.; Škorić, I. Identification Of Degradation Products Of Praziquantel During The Mechanochemical Activation. *Journal of Pharmaceutical and Biomedical Analysis* 2018, *159*, 291-295.

[11] Devogelaer, J.; Charpentier, M.; Tijink, A.; Dupray, V.; Coquerel, G.; Johnston, K.; Meekes, H.; Tinnemans, P.; Vlieg, E.; ter Horst, J.; de Gelder, R. Cocrystals Of Praziquantel: Discovery By Network-Based Link Prediction. *Crystal Growth & Design* 2021, *21* (6), 3428-3437.

[12] Yang, D.; Cao, J.; Heng, T.; Xing, C.; Yang, S.; Zhang, L.; Lu, Y.; Du, G. Theoretical Calculation And Structural Analysis Of The Cocrystals Of Three Flavonols With Praziquantel. *Crystal Growth & Design* 2021, *21* (4), 2292-2300.

[13] Shemchuk, O.; Grepioni, F.; Braga, D. Mechanochemical Preparation And Solid-State Characterization Of 1:1 And 2:1 Ionic Cocrystals Of Cyanuric Acid With Alkali Halides. *Crystal Growth & Design* 2020, *20* (11), 7230-7237.

[14] Gomollón-Bel, F. Ten Chemical Innovations That Will Change Our World: IUPAC Identifies Emerging Technologies In Chemistry With Potential To Make Our Planet More Sustainable. *Chemistry International* 2019, *41* (2), 12-17.

[15] Friščić, T.; Mottillo, C.; Titi, H. Mechanochemistry For Synthesis. *Angewandte Chemie International Edition* 2019, *59* (3), 1018-1029.

[16] Hernández, J.; Bolm, C. Altering Product Selectivity By Mechanochemistry. *The Journal of Organic Chemistry* 2017, *82* (8), 4007-4019.

[17] Macrae, C.; Bruno, I.; Chisholm, J.; Edgington, P.; McCabe, P.; Pidcock, E.; Rodriguez-Monge, L.; Taylor, R.; van de Streek, J.; Wood, P. Mercury CSD 2.0– New Features For The Visualization And Investigation Of Crystal Structures. *Journal of Applied Crystallography* 2008, *41* (2), 466-470.

[18] Bruker AXS: SAINT+, release 6.22. Bruker Analytical Systems: Madison,WI. 2005.

[19] Bruker AXS:SADABS. Bruker Analytical Systems: Madison,WI. 2005.

[20] Sheldrick GM. A short history of SHELX. Acta Crystallographica Section A. 2008;64:112-22.

[21] Farrugia LJ. WinGX - Version 1.80.05. J Appl Cryst. 1999;32:837-8.

[22] Spek A.L. Single-crystal structure validation with the program PLATON. Journal of Applied Crystallography. 2003;36:7-13.

[23] Praziquantel: Uses, Interactions, Mechanism of Action DrugBank Online. https://www.drugbank.ca/drugs/DB01058 (accessed Oct 14, 2021).